Proceedings of 8th Windsor Conference: ***Counting the Cost of Comfort in a changing world*** Cumberland Lodge, Windsor, UK, 10-13 April 2014. London: Network for Comfort and Energy Use in Buildings, http://nceub.org.uk

Field evaluation of the performance of a radiant heating/cooling ceiling panel system

Ryozo Ooka[1], Rongling Li [2], Togo Yoshidomi [2] and Bjarne W. Olesen[3]

1 Institute of Industrial Science, the University of Tokyo, 4-6-1 Komaba, Meguro-ku, Tokyo, Japan, ooka@iis.u-tokyo.ac.jp

2 Graduate School of Engineering, the University of Tokyo

3 Intl. Centre for Indoor Environment and Energy, Technical University of Denmark

Abstract

For testing different engineering solutions for energy-efficient buildings, a low-energy building was built at the University of Tokyo as a pilot project. In this building, a radiant heating/cooling ceiling panel system is used. This study aims to not only clarify the system performance but also to share our experience and results for them to serve as a reference for other similar projects. Here, the system performance in relation to its heating/cooling capacity and thermal comfort has been evaluated. The heat transfer coefficient from water to room was 3.7 W/(m^{2}K) and 4.8 W/(m^{2}K) for heating and cooling, respectively. The thermal comfort measurement showed that the air and operative temperature distributions in the room were highly uniform. In both heating and cooling, the PMV was higher than -0.5 and less than +0.5 and the PPD was less than 10%. A category B thermal environment was obtained using the radiant ceiling heating/cooling system.

Keywords: Radiant heating/cooling ceiling; overall heat transfer coefficient; heat use efficiency; thermal comfort; in situ

1. Basic theory

Figure 1 shows the cross section of the testing room with a suspended ceiling. In this figure, θ_S is the mean surface temperature of the radiant panels; θ_u, the mean air temperature of the plenum; θ_o, the room's operative temperature as measured in its middle at a height of 0.7 m above the floor; θ_w, the mean heating/cooling water temperature; q_W, the heating/cooling capacity of water [W/m^2]; q_1, the heat flux from the water to the room [W/m^2]; and q_2, the heat flux from the water to the plenum [W/m^2].

This study aims to evaluate the in situ performance of the system, including the overall heat transfer coefficient from the water to the room U_{wo} and from the water to the plenum U_{wu}, and to analyze the heat loss. Because no standard exists for the evaluation of in situ radiant heating/cooling ceiling panel systems, we create a resistance model for the radiant ceiling according to ISO 11855-2 (2012) and EN 14240 (2004). This model is shown in Figure 2, and it is governed by the following equations:

$$\theta_w = (\theta_{w,in} + \theta_{w,out})/2 \quad (1)$$

$$U_{wo} = q_1 /(\theta_w - \theta_o) \quad (2)$$

$$U_{wu} = q_2 /(\theta_w - \theta_u) \quad (3)$$

$$q_2 = q_w - q_1 \quad (4)$$

$$q_w = \rho cm(\theta_{w,in} - \theta_{w,out}) / A_p \quad (5)$$

$$R_{wo} = 1/U_{wo} \quad (6)$$

$$R_{wu} = 1/U_{wu} \quad (7)$$

Here, $\theta_{w,in}$ and $\theta_{w,out}$ are the supply and return water temperatures, respectively [°C]; m is the water flow rate [m^3/h]; ρ and c are the water density [kg/m^3] and specific heat capacity of water [kJ/(kgK)], respectively; A_p is the area of the panels [m^2]; R_{ws} is the thermal resistance between the fluid and the radiant panel surface; R_{so} and R_{su} are the thermal resistances from the panel surface to the room and the plenum, respectively; and R_{wo} and R_{wu} are the thermal resistances between the water and the room and between the water and the plenum, respectively. The unit of thermal resistance is [m^2K/W].

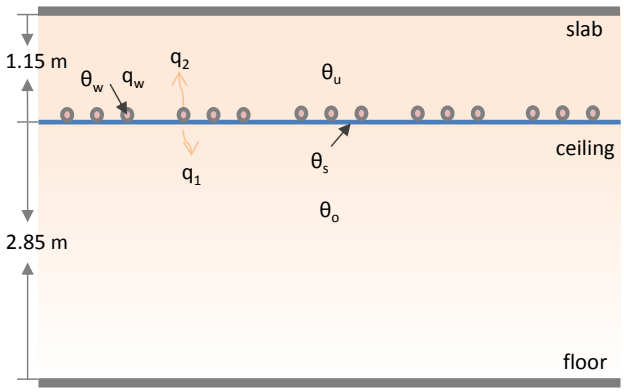

Figure 1 Cross section of testing rooms

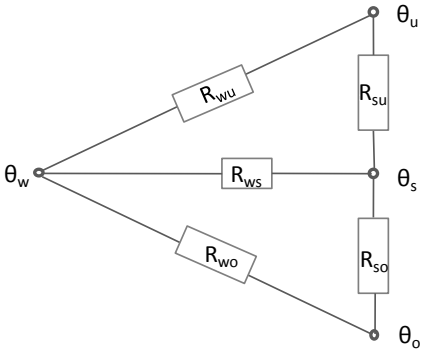

Figure 2 Resistance model for radiant panel

To verify the accuracy of the measurements, we followed ISO 11855-2. The ISO 11855 series is applicable to water-based embedded surface heating and cooling systems in residential, commercial, and industrial buildings, and it is applicable to systems integrated into the wall, floor, or ceiling construction without any open air gaps because the heat transfer coefficient between the radiant surface and the room is not related to the structure of the radiant body. The recommended heat transfer coefficient can be used as a reference value for our study. This standard recommends theoretical models for calculating the heat flux between the ceiling and the room as

$$q_1 = U_{so}(\theta_s - \theta_o) \quad (8)$$

Here, U_{so} is the heat transfer coefficient between the radiant surface and the room, which combines convection and radiation. Its value is 6 W/(m^2K) for ceiling heating systems. For ceiling cooling systems, it is given as follows:

$$q_1 = 8.92(\theta_s - \theta_o)^{1.1} \quad (9)$$

2. Test description

2.1 Testing system

The tested radiant cooling/heating panel ceiling system consists of aluminum panels (area: 1.26 m^2 (2.1 m × 0.6 m)) that are coated on the bottom surface, as shown in Figure 3. The main characteristics of the radiant panel are presented in Table 1. Although holes are present on the surface of the panel, a black painted aluminum board is placed behind the entire panel, and the areas of the holes are included in the calculation of the radiant area. Above the aluminum board, the entire suspended ceiling is covered with insulation to prevent upward heat flux entering the plenum.

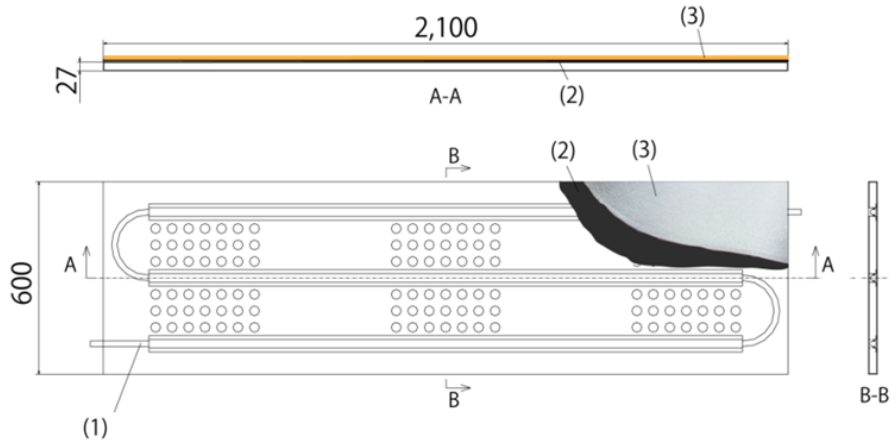

(1) Polybutene pipe (2) Aluminum board (3) Insulation board
Figure 3 Radiant panel

Table 1 Main characteristics of tested radiant panel

	characteristic
(1)	polybutene; internal diameter: 13 mm, external diameter: 18 mm
(2)	0.25 mm
(3)	10 mm glass wool

2.2 Testing room

Classrooms M and L on the 4th floor of 21KOMCEE were used as testing rooms (Ryozo et al, 2013). Figure 4 shows the position and floor plan of the testing rooms. The ceiling area of classroom M is 103.7 m^2, with 45% area covered by panels. The ceiling area of classroom L is 174.1 m^2, with 40% area covered by panels.

Each room has one hydronic system, and these two systems are connected in parallel to a water-to-water heat exchanger, where the water of the panel system exchanges heat with the hot/cold water from the energy supply. As seen in Fig. 6, the supply/return water temperatures and the water flow rate are measured at the outlet/inlet of the heat exchanger by sensors TE-1, TE-2, and FM, respectively. Because the conditions in the two rooms were identical during the measurements, their supply/return water temperatures were assumed to be identical. Here, classroom M was chosen as the main room for measurement.

Figure 5 shows the ceiling description and the panel positions in classroom M. 72 panel units (2100 × 600 mm) are installed in three parallel modules.

The dimensions of classroom M are as follows:
Length: 10.8 m (Figure 5)

Width: 9.6 m (Figure 5)
Height: 2.85 m (below ceiling)
Height of ceiling plenum: 1.15 m (above ceiling)

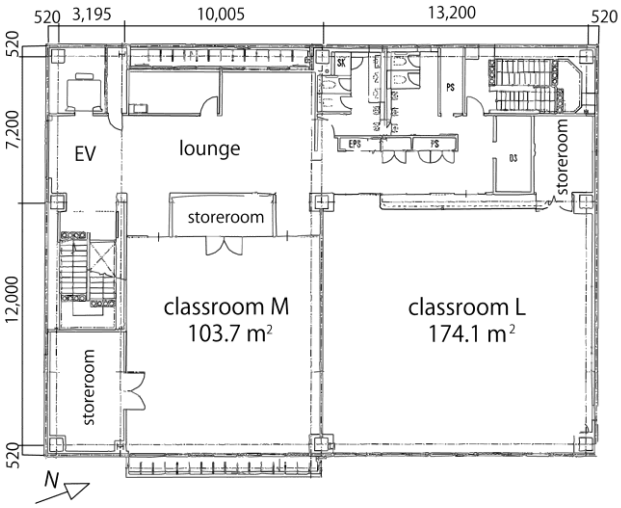

Figure 4 Testing room position and floor plan

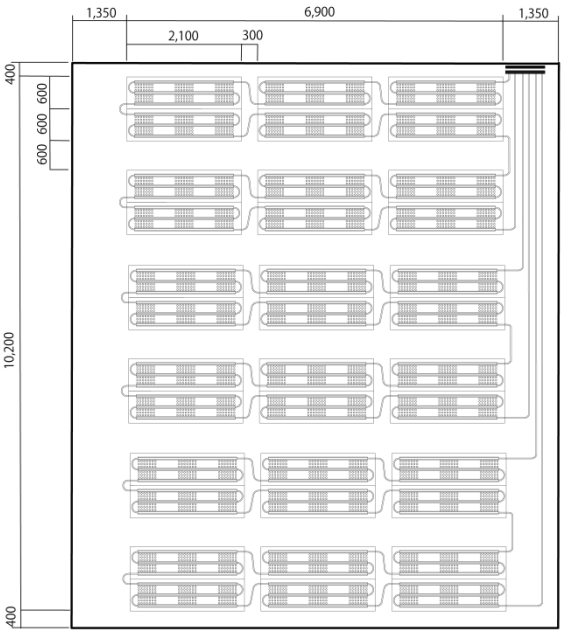

Figure 5 Ceiling description and panel positions in classroom M

The building has a well-insulated reinforced concrete structure. The external wall of room M faces east, and the wall has a double skin system with movable louvers. This system's U value has been measured to be 1.45 W/(m^2K) (Shida et al, 2012).

2.3 Water circuit control

The supply water flow rate and temperature were controlled during the measurements. Figure 6 shows the water loop. The supply water flow rate and temperature were controlled by adjusting the position of valves MV-1 and MV-2, respectively. MV-2 is a volume control valve of the water loop that is connected with the heat supply equipment.

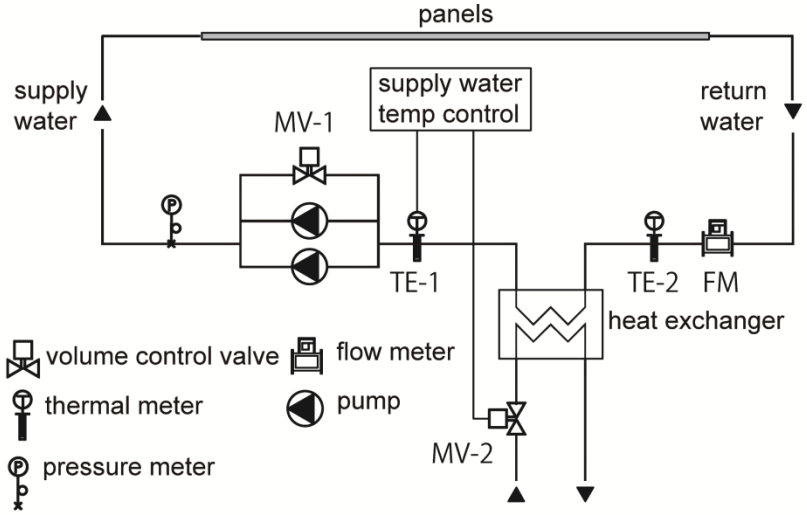

Figure 6 Water hydraulic system control

2.4 Instruments and sensors

As seen in Figure 7, sensors were placed at positions 1 to 7 in room M and a θ_o sensor was placed at position 8 in room L. Table 2 lists the instruments and sensors used in the measurements. For our measurements, we used thermography to check the surface temperature profiles of the ceiling and to find suitable locations for the thermocouple sheets (THSs) and heat flux meters (HFMs). From the thermographs of each panel, we observed that the temperature at the center of the panel was equal to the average temperature of the entire panel. Thus, we decided to place the sensors at the centers of the panels, as seen at locations 1, 2, 3, and 4 (Figure 7 (b)). HFMs were pasted on the panel surfaces to measure both the surface temperature θ_s and heat flux q_1. To verify the accuracy of the measured values, THSs were also pasted at locations 1, 3, and 4 for data comparison. At the center of the room, location 5, we set 6 thermocouples at 0.1 m, 0.7 m, 1.1 m, and 1.7 m above floor level, 0.1 m below ceiling, and 0.1 m above ceiling to measure the vertical air temperature profile. Because a 3-to-5-cm-diameter grey globe sensor accurately presents the operative temperature θ_o, we used 4-cm grey painted ping-pong balls as operative temperature sensors (Simone, 2007; ISO 7726, 1998). To obtain the horizontal profile of θ_o, we placed the globe sensors 0.7 m above the floor level at the center of the room (location 5), on the window side (location 6), and at the corner of an interior wall (location 7).

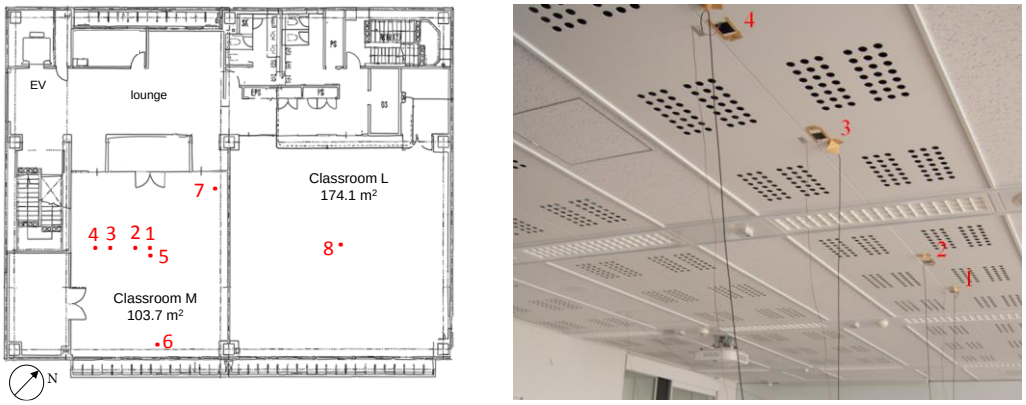

(a) Sensor locations (b) Radiant ceiling panel system and sensors

Figure 7 Sensors and locations

Table 2 Instruments and sensors

Instrument/sensor	Measurement	accuracy
Thermocouple sheet (THS)	Surface temperature	±0.5°C
Heat flux meter (HFM)	Surface temperature & heat flux	±0.01°C ±0.01 W/m^2
Thermography	Surface temperature	±2.0°C
Thermocouple	Vertical air temperature profile	±0.5°C
Globe sensor	Horizontal operative temperature profile	±0.5°C
Pt100	Water temperature	JIS(1997) class A ±(0.15 + 0.002| t |)°C
Electromagnetic flow meter	Water flow rate	0.25–0.5% of rate

Measurements of the supply water mass flow rate, supply water temperature, return water temperature, and ambient temperature were performed using the sensors of the building management system.

2.5 Measurement protocol

The heating mode measurements were carried out during March 18–23, 2013. Because the outdoor temperature was almost 20°C during the daytime, it was too warm to operate the heating system. It was also desirable to avoid interference from solar radiation. Thus, the measurements were carried out during the night time from 19:00 to 7:00. The cooling mode measurements were carried out during September 10–13, 2013, from 8:00 to 17:00. Table 3 lists the cases and outdoor temperatures during the measurements. H1–H4 are the heating measurement cases and C1–C3 are the cooling cases.

Table 3 Cases & outdoor temperature

	H1	H2	H3	H4	C1	C2	C3
supply water temperature [°C]	40	40	28	35	18	18	20
water flow rate [m^3/*h*]	2.0	2.0	2.0	2.0	2.0	2.0	2.0
outdoor temperature [°C]	16–20	7–13	13–17	12–16	26–32	23–28	28–32

3. Results

The data collected in the steady state (EN 14240, 2004) are used for the analysis.

3.1 Heat flux and heat transfer coefficient

(1) Heat flux measurements and uncertainty analysis

The heat flux q_1 was measured using HFMs and calculated using Eq. (8) for heating mode and Eq. (9) for cooling mode, respectively. The result of this calculation was compared with the experimental data to validate the measurements. Figure 8 (a) shows the steady state (23:00 to 6:00) values for H2 and (b) shows the steady state (12:00 to 17:00) values for C3. For case H2, the mean value of the measured heat flux ($q_{1,meas}$ in the figure) is 50.8 W/m^2, and the heat flux calculated from Eq. (8) ($q_{1,calc}$ in the figure) is 49.0 W/m^2. In the calculation, θ_s is the mean value of the temperatures measured at locations 1–4 and θ_o is measured at location 5.

Table 4 lists the measurement results for all the cases. The differences between $q_{1,meas}$ and $q_{1,calc}$ are less than 4% for H1, H2, and H4 and ~7% for cases C1–C3. Good agreement was found between the theoretical heat flux and the measured data.

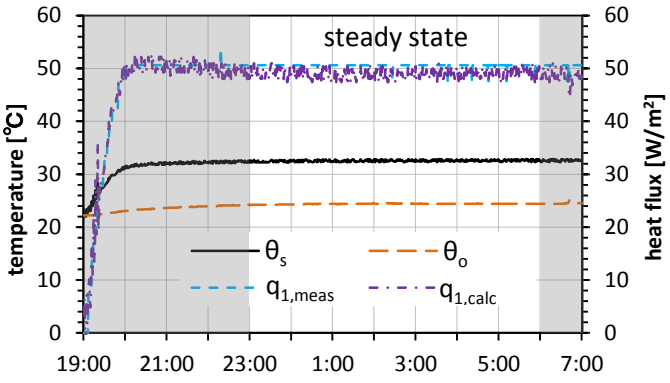

(a) H2

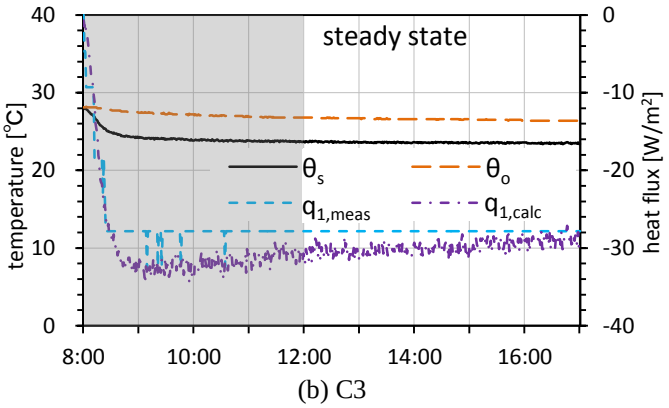

(b) C3

Figure 8 Measurement results and calculation results for heat flux

The deviation for H3 is significant and that for cases C1–C3 is higher than in the three heating cases. To clarify the reason for this, the measurement uncertainty is evaluated according to the JCGM 100 (2008) standard. Considering the accuracy provided by the instrument specifications is type B uncertainty and taking into account a coverage factor of 2, the combined uncertainty is calculated. For the temperature difference $\theta_s - \theta_o$, it is ±0.5°C, and for the measurement heat flux $q_{1,meas}$, it is ±0.02 W/m^2. The uncertainty of $\theta_s - \theta_o$ then translates into the uncertainty of $q_{1,calc}$, which is given

by Eqs. (8) and (9). As a result, $q_{1,calc}$ has a distribution with upper and lower bounds of ±3.0 W/m^2 for heating cases and approximately ±6.0 W/m^2 for cooling cases.

Table 4 Accuracy of measured heat flux

	H1	H2	H3	H4	C1	C2	C3
$\theta_s - \theta_o$ [°C]	8.2	8.2	2.5	5.9	-3.7	-3.4	-3.0
Measurement heat flux $q_{1,meas}$ [W/m^2]	49.8	50.8	18.2	35.0	-35.4	-32.0	-27.8
Calculated heat flux $q_{1,calc}$ [W/m^2]	49.0	49.0	15.0	35.3	-38.0	-34.5	-30.0
Relative deviation $\lvert q_{1,meas} - q_{1,calc} \rvert / q_{1,calc}$	1.6%	3.6%	21.2%	0.8%	7.0%	7.2%	7.3%

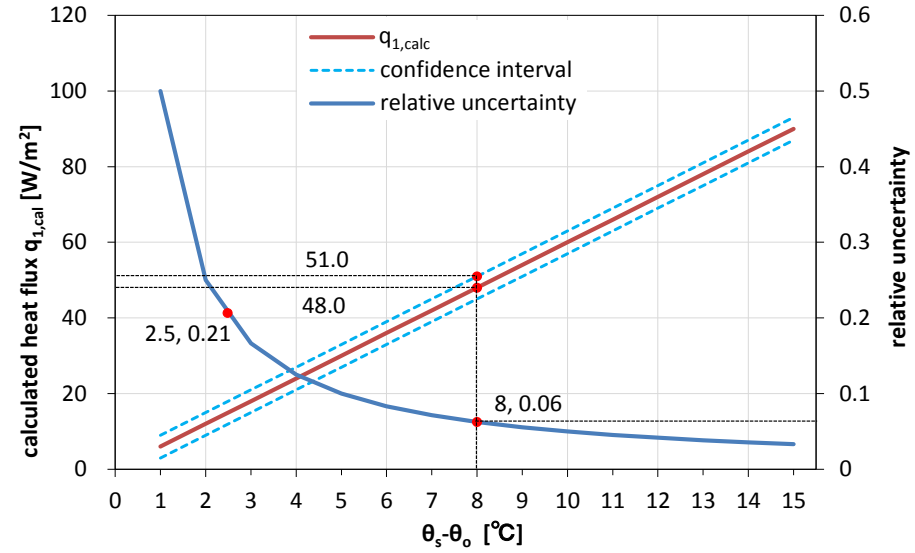

(a) Heating mode

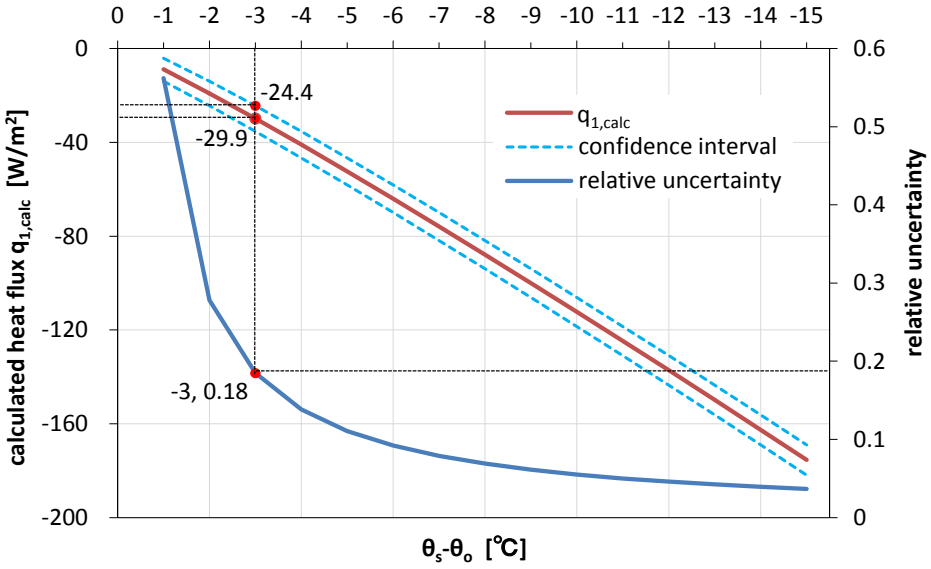

(b) Cooling mode

Figure 9 Relative uncertainty of calculated heat flux $q_{1,calc}$

Fig. 9 shows the relative uncertainty (ratio of uncertainty to $q_{1,calc}$) of the calculations. It is obvious that as the temperature difference $\theta_s - \theta_o$ decreases, the relative uncertainty of $q_{1,calc}$ increases. The red points in Figure 9 (a) show the relative uncertainty, where $\theta_s - \theta_o$ is 8°C and 2.5°C, respectively. The relative uncertainty at 8°C is (51.0-48.0)/48.0 = 0.06 and that at 2.5°C is 0.21. Figure 9 (b) shows that the relative uncertainty at -3°C for cooling cases is 0.18. Because the relative uncertainty increases when the absolute temperature difference decreases, the accuracy of $q_{1,calc}$ reduces from H1, H2, H4, C1–C3, to H3. This could explain the increase in the relative deviation.

This result indicates that ISO 11855-2 can also be applied to suspended ceiling systems; however, the accuracy is reduced when the temperature difference between the radiant surface and the room decreases. Thus, it is necessary to use very accurate sensors when the temperature difference is small.

(2) Heat flux and heat transfer coefficient

Table 5 lists the measurement results for the heat flux q_1 and overall heat transfer coefficient U_{wo}. In the testing room, the space above the ceiling is a plenum connected to an exhaust system. Therefore, the heat flux to the above space q_2 could be heat loss. The downward heat flux ratio of q_1/q_w can be considered an indicator of the heat use efficiency in the occupied room. Its value was 61–65% for H1, H2, and H4 and 65–72% for C1–C3. This result indicates that the heat flux in the upward direction is 30–40% with the exhaust system in operation; this could be considered heat loss.

For H3, with a supply water temperature of 28°C, the downward heat flux ratio increased to 83% and the upward heat flux reduced to 17%.

The overall heat transfer coefficient U_{wo} is ~3.7 W/(m^{2}K) for H1, H2, and H4 and 4.2 W/(m^{2}K) for H3. For cooling mode, U_{wo} is 4.7–4.9 W/(m^{2}K), which is higher than in the heating cases.

Table 5 Measurement results for heat flux and heat transfer coefficient

	H1	H2	H3	H4	C1	C2	C3
$\theta_w - \theta_o$ [°C]	14.0	13.6	4.3	9.6	-7.2	-6.8	-5.7
q_w [W/m^2]	82.0	78.6	21.8	54.8	-51.0	-49.1	-38.8
q_1 [W/m^2]	49.8	50.80	18.2	35.0	-35.4	-32.0	-27.8
Downward heat flux ratio q_1/q_w	61%	65%	83%	64%	69.3%	65.2%	71.8%
U_{wo} [W/(m^{2}K)]	3.6	3.7	4.2	3.7	4.9	4.7	4.9

3.2 Thermal comfort

The desired thermal environment for the classroom is category B according to ISO 7730 (2005). Table 6 shows the limits of factors in category B.

Table 6 Factors of thermal environment Category B

PPD%	PMV	Vertical air temperature difference	Radiant asymmetry	PD% Caused by warm or cool floor	DR%
< 10	-0.5 < PMV < +0.5	< 5	< 5	< 10	< 20

(1) PD% and DR%

PD% is the percentage of people dissatisfied by the floor temperature which is estimated by a function given in ISO 7730. The floor temperature of the classroom was about 27°C and 24°C in cooling time and heating time, respectively. For these temperatures ISO 7730 gives a PD% that is less than 10%. DR% is the percentage of people predicted to be bothered by draught. An estimate relationship between air velocity and DR% is recommended in ISO 7730. Due to only radiant ceiling panel system was used during the measurements, the air velocity was weak. The indoor air velocity was less than 0.03 m/s which gives a DR% much lower than 20%.

(2) Indoor temperature distribution

Figure 10 shows the indoor temperature distributions for H2 and C3. The vertical air temperature difference between 0.1 m and 1.7 m is less than 1.5°C. The θ_o difference from the window side to the center of the room and to the internal corner is also less than 1.5°C. The air temperature and θ_o distributions in the room were highly uniform, which contributes toward a category B thermal environment.

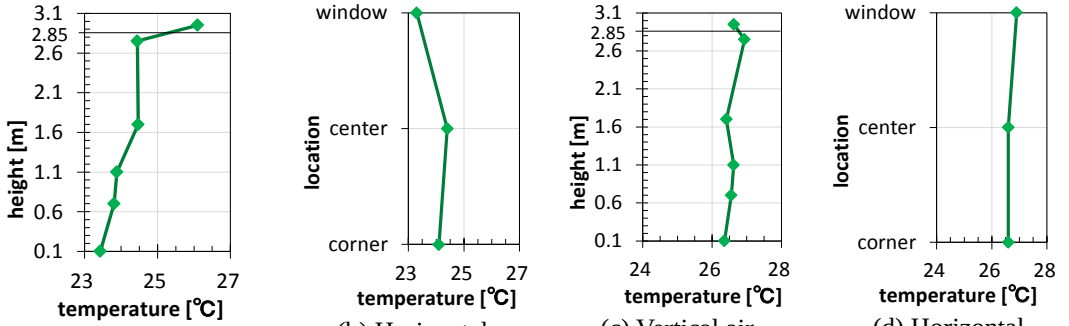

(a) Vertical air temperature distribution (H2)

(b) Horizontal operative temperature distribution (H2)

(c) Vertical air temperature distribution (C3)

(d) Horizontal operative temperature distribution (C3)

Figure 10 Indoor temperature distribution

(3) PMV and PPD

Figure 11 shows the PMV and PPD for H2 and C3. For the calculation Met was 1.1 and clo was 0.3 for summer and 1.0 for winter. In both heating and cooling, the PMV was higher than -0.5 and less than +0.5, the PPD was less than 10%.

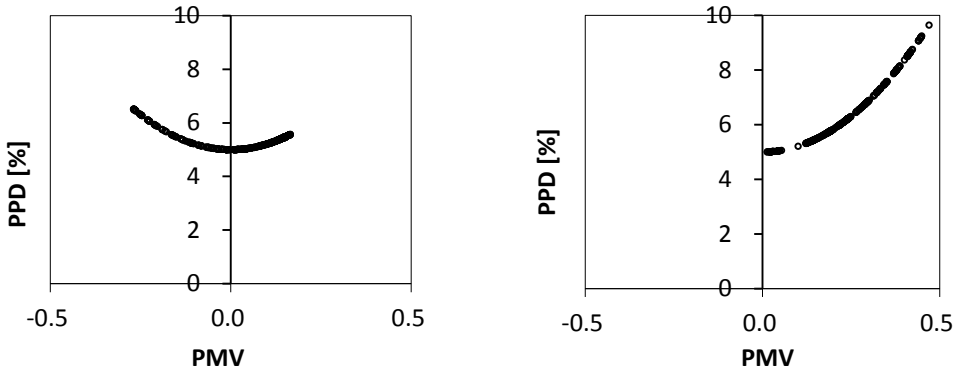

(a) H2 (b) C3

Figure 11 PMV and PPD

All the criteria are satisfied simultaneously and the category B thermal environment was obtained using the radiant ceiling heating/cooling system.

4. Discussion and conclusion

Good agreement was found between the theoretical heat flux and the measured data. The relative deviation is less than 4% for the heating mode and ~7% for the cooling mode. The deviations for the cooling cases are larger than those for the heating cases. This is because during the cooling measurements, the relative uncertainty of the measurement heat flux was much larger than in the heating mode. This indicates that ISO 11855-2 can be applied to suspended ceiling systems; however, its accuracy reduces as the temperature difference between the radiant surface and the room decreases. Thus, it is necessary to use very accurate sensors when the temperature difference is small.

The overall heat transfer coefficient U_{wo} was ~3.7 W/(m^{2}K) and 4.8 W/(m^{2}K) for heating mode and cooling mode, respectively. The downward heat flux ratio q_1/q_w was 61–65% for heating mode and 65–72% for cooling mode. This shows that the upward heat flux is approximately 30–40% while the exhaust system is operating; this could be considered heat loss. The upward heat flux was large, especially during heating cases. The insulation above the panels should be improved to reduce the upward heat loss. In addition, using the plenum as an air supply "duct" could also reduce the heat loss by bringing the heat into the room with the supply air.

With regard to heating cases, it was obvious that the performance of case H3 was different from that of other cases in light of the much lower water temperature (Tables 3 and 5). For H3, the upward heat flux, which is the potential heat loss, was 17%, which was half that in other cases. However, the heating capacity reduced dramatically to ~22 W/m^2. An optimal water temperature is assumed to exist with high heat use efficiency and sufficient heating capacity. Furthermore, because the heating loads vary with the weather, the water temperature should not be constant.

The air temperature difference between 0.1 m to 1.7 m was less than 1.5°C in both heating and cooling modes; furthermore, the θ_o distribution at 0.7 m level was no more than 1.5°C. The room temperature was highly uniform. In both heating and cooling, the PMV was higher than -0.5 and less than +0.5, the PPD was less than 10%. A category B thermal environment was obtained using the radiant ceiling heating/cooling system.

Acknowledgments
The authors would like to thank Tomonari Yashiro, Bumpei Magorio, Hiroshi Sako, et al., the collaborators of the reported experimental building. The authors acknowledge the funding agencies including NEDO for their support and contribution.

References

Kolarik J, Toftum J, Olesen BW, Jensen KL, 2011. Simulation of energy use, human thermal comfort and office work performance in buildings with moderately drifting operative temperatures. *Energy and Buildings*, 43:2988-2997.

Olesen BW, 2002. Radiant floor heating in theory and practice. ASHRAE Journal.

Okamoto S, Kitora H, Yamaguchi H, Oka T, 2010. A simplified calculation method for estimating heat flux from ceiling radiant panels. Energy and Buildings, 42:29-33.

Olesen BW, 2011. Radiant heating and cooling by embedded water-based systems. I Congreso Clima2011plus.

Ooka R, Yashiro T, et al. 2013, Zero Energy Building Project in the University of Tokyo. CLIMA 2013, Prague.

Causone F, Corgnati SP, Filippi M, Olesen BW, 2009. Experimental evaluation of heat transfer coefficients between radiant ceiling and room. Energy and Buildings, 41:622-628.

Karadag R, 2009. The investigation of relation between radiative and convective heat transfer coefficients at the ceiling in a cooled ceiling room. Energy Conversion and Management, 50.

Zhang L, Liu X-H, Jiang Y, 2013. Experimental evaluation of a suspended metal ceiling radiant panel with inclined fins. Energy and Buildings 2013, 62:522-5299.

Jeong J-W, Mumma SA, 2003. Ceiling radiant cooling panel capacity enhanced by mixed convection in mechanically ventilated spaces. Applied Thermal Engineering, 23:2293-2306.

Diaz NF, Lebrun J, Andre P, 2010. Experimental study and modeling of cooling ceiling systems using steady-state analysis. Refrigeration, 33:793-805.

Fonseca N, 2011. Experimental study of thermal condition in a room with hydronic cooling radiant surface. Refrigeration, 34:686-695.

Jeong J-W, Mumma SA, 2004. Simplified cooling capacity estimation model for top insulated metal ceiling radiant cooling panels. Applied Thermal Engineering , 24:2055-2072.

ISO 11855-2. 2012. Building environment design－Design, dimensioning, installation and control of embedded radiant heating and cooling systems－Part 2: Determination of the design heating and cooling capacity. International Organization for Standard, Genève, Switzerland.

EN 14240. 2004. Ventilation for buildings－Chilled ceilings－Testing and rating. European Committee for Standardization, Brussels, Belgium.

ANSI/ASHRAE Standard 138-2009. 2009. Method of testing for rating ceiling panels for sensible heating and cooling. American Society of Heating, Refrigerating and Air-conditioning Engineers, Inc., Atlanta, USA

EN 14037-1. 2003. Ceiling mounted radiant panels supplied with water at temperature below 120°C. European Committee for Standardization, Brussels, Belgium.

Shida H, Ooka R, et al. 2012, ZEB-oriented Project in University Campus (part 5) Development and performance validation of simple double-skin configured by movable louver. The Summaries of Technical Papers of Annual Meeting 2012, Architectural Institute of Japan.

Simone A, Babiak J, Bullo M, Landkilde G, Olesen BW, 2007. Operative temperature control of radiant surface heating and cooling systems. Proceedings of Clima 2007 Wellbeing Indoors.

ISO 7726. 1998. Ergonomics of the thermal environment－Instruments for measuring physical quantities. International Organization for Standard, Genève, Switzerland.

JIS C1604-1997. Resistance thermometer sensors. Japanese Industrial Standards, Tokyo, Japan.

JCGM 100: 2008 GUM 1995 with minor corrections. 2008. Evaluation of measurement data－Guide to the expression of uncertainty in measurement.

ISO 7730. 2005. Ergonomics of the thermal environment－Analytical determination and interpretation of thermal comfort using calculation of the PMV and PPD indices and local thermal comfort criteria. International Organization for Standard, Genève, Switzerland.

Nomenclature

θ_s	mean surface temperature of the radiant panels [°C]
θ_u	mean temperature of the plenum space [°C]
θ_o	operative temperature measured in the middle of the room at 0.7 m above the floor [°C]
θ_w	mean heating/cooling water temperature [°C]
q_w	heating/cooling capacity of the water [W/m^2]
q_1	heat flux from the water to the room [W/m^2]
q_2	heat flux from the water to the plenum [W/m^2]
$q_{1,meas}$	measurement heat flux [W/m^2]
$q_{1,calc}$	calculated heat flux [W/m^2]
$\theta_{w,in}$	supply water temperature [°C]
$\theta_{w,out}$	return water temperature [°C]
m	water flow rate [m^3/h]
ρ	water density [kg/m^3]
c	specific heat capacity of the water [kJ/(kgK)]
R_{ws}	thermal resistance between the fluid and the panel surface [m^{2}K/W]
R_{so}	thermal resistance from the panel surface to the room [m^{2}K/W]
R_{su}	thermal resistance from the panel surface to the plenum [m^{2}K/W]
R_{wo}	thermal resistance between the water and the room [m^{2}K/W]
R_{wu}	thermal resistances between the water and the plenum [m^{2}K/W]
U_{wo}	overall heat transfer coefficient from the water to the room [W/(m^{2}K)]
U_{wu}	overall heat transfer coefficient from the water to the plenum [W/(m^{2}K)]
U_{so}	heat transfer coefficient between the radiant surface and the room [W/(m^{2}K)]